Catalysis Today 154 (2010) 229–236

Contents lists available at ScienceDirect

Catalysis Today

journal homepage: www.elsevier.com/locate/cattod

A comparative study on catalyst deactivation of nickel and cobalt incorporated MCM-41 catalysts modified by platinum in methane reforming with carbon dioxide

Dapeng Liu[a], Wei Ni Evelyn Cheo[a], Yi Wen Yvonne Lim[a], Armando Borgna[b], Raymond Lau[a], Yanhui Yang[a,*]

[a] School of Chemical and Biomedical Engineering, Nanyang Technological University, 62 Nanyang Drive, Singapore 637459, Singapore
[b] Institute of Chemical and Engineering Sciences (ICES), A*STAR, 1 Pesek Road, Jurong Island, Singapore 627833, Singapore

ARTICLE INFO

Article history:
Available online 24 April 2010

Keywords:
Methane reforming with CO_2
Co-MCM-41
Ni-MCM-41
Pt promotion

ABSTRACT

Methane dry reforming with CO_2 over Pt modified Co- and Ni-MCM-41 was comparatively studied. The incorporation of Co and Ni ions was completed by direct hydrothermal method while Pt was introduced by conventional wet impregnation. The catalytic results showed the introduction of an appropriate amount of Pt exhibited a higher activity compared to the unmodified Co- and Ni-MCM-41 catalysts. In the long-term stability test, Pt impregnated Ni-MCM-41 gave the highest conversion and catalytic stability, while a remarkable decrease of catalytic activity was observed over Pt impregnated Co-MCM-41, which was also lower than that of Pt impregnated MCM-41. The effect of Pt was suggested to be due to its lower tendency to carbon deposition. Characterization results showed a strong interaction between Pt and Co or Ni which facilitated the improvement of catalytic performance.

1. Introduction

The increased emissions of greenhouse gases (GHG) such as carbon dioxide (CO_2), methane (CH_4) and nitrous oxide (N_2O) in the atmosphere have become major environmental problems leading to global climate change. This situation heightened the interest worldwide for the control, conversion and utilization of GHG [1–3]. Under such circumstances, CH_4 reforming with CO_2 to produce synthesis gas, namely, a mixture of CO and H_2, attracted renewed interest based on the utilization of CO_2 and production of synthesis gas, a useful intermediate for producing hydrocarbon fuels and valuable oxygenated chemicals [4–6].

The reforming of CH_4 with CO_2 has been extensively studied on supported group VIII metal catalysts. Both noble metals (e.g. Ru, Rh, Pd, Pt, Ir) and non-noble metals (e.g. Ni, Co, Fe) were found to be catalytically active towards this reaction [7]. The noble metal exhibits the important advantage of being active with low carbon deposition. The drawback of noble metal catalysts is their high cost and limited availability. In contrast, non-noble metals are less expensive and widely available. However, dry reforming being strongly endothermic requires high temperatures (typically 800–900 °C) and this leads to the rapid deactivation of the catalyst by carbon deposition and/or metal sintering for non-noble metals when the active metals are incorporated/impregnated into conventional supports such as Al_2O_3, SiO_2, MgO [7–10].

Several interesting observations were reported on introducing noble metals to Ni catalysts for dry reforming of methane [11]. A significant enhancement in catalytic activity and stability was found by adding Pt, Pd and Rh to a $Ni_{0.03}Mg_{0.97}O$ catalyst [12]. Over SiO_2 supported Ni–Rh catalysts, the effective formation of a Ni–Rh alloy can easily take place, but only the Rh-rich catalysts were resistant against deactivation and coke deposition [13]. NiY and Niβ monometallic catalysts were almost inactive in comparison with zeolite supported Pt and Pt–Ni catalysts [14]. Furthermore, the excellent catalytic activity of BEA support was attributed to its open structure, weak acidity, therefore leading to the low tendency of coking. A remarkable influence on the catalytic performance was reported as Ru was added to supported Ni catalysts [15]. The improvement of Ru was more pronounced in the case of SiO_2 than H-ZSM-5, which was ascribed to the increased metallic dispersion of Ni as a consequence of the formation of Ni–Ru clusters with a Ni enriched surface. Indeed, by alloying Au into Ni surface layer, the supported Ni catalyst was more robust and essentially no deactivation was found in the steam reforming of *n*-butane [16], implying the presence of Au atoms at low-coordination sites blocked the adsorption of C atoms, and thus significantly preventing the formation of carbon whiskers [17].

In contrast to microporous zeolites and conventional macroporous materials, mesoporous molecular sieve, as a novel support material, has distinct advantages such as nanometer-sized pore

* Corresponding author. Tel.: +65 6316 8940; fax: +65 6794 7553.
E-mail address: yhyang@ntu.edu.sg (Y. Yang).

0920-5861/$ – see front matter © 2010 Elsevier B.V. All rights reserved.
doi:10.1016/j.cattod.2010.03.054

structures, high surface area and adjustable metal composition and types, providing good opportunities to develop novel catalysts with improved catalytic performance [18,19]. In our previous studies, Ni-containing mesoporous molecular sieves, such as Ni-incorporated MCM-41, Ni-grafted SBA-15 exhibited good catalytic performances in dry reforming [20,21]. Furthermore, we observed superior activity of Ni–Zr-MCM-41 among a series of Ni-based bimetallic MCM-41 catalysts [22].

In the present contribution, the effect of impregnating a small amount of noble metal Pt on the catalytic properties of Co-MCM-41 and Ni-MCM-41 in dry reforming is investigated. Combining the good carbon-resistance of noble metal Pt and suitable activity of non-noble metal Co or Ni, the goal is to attain an improved catalytic performance for CO_2 dry reforming.

2. Experimental

2.1. Catalysts preparation

Transition metal incorporated MCM-41 materials were synthesized according to a modified procedure reported by Lim et al. [23]. Co-MCM-41 was synthesized with the molar ratio of $1SiO_2$:0.27Surfactant:0.26NaOH:0.04Co:$70H_2O$. In a typical synthesis, the surfactant solution was prepared by mixing 2.95 g of hexadecyltrimethyl-ammonium bromide (CTAB, >99%, Sigma), 0.31 g of sodium hydroxide (NaOH, >98%, Fluka) and 9.8 g distilled water at 40 °C until a clear solution was obtained. In a separate beaker, silica precursor was prepared by mixing 1.28 g of fumed silica (Cab-O-Sil, M5, 99.8%, Sigma), 5.25 g of tetramethylammonium silicate (20%, Aldrich) and 9.8 g of distilled water were mixed for 30 min. Cobalt (II) sulphate ($CoSO_4 \cdot 7H_2O$, >99%, Sigma) was added to the silica precursor solution and stirred for 1 h. The surfactant solution was then added followed by adding two drops antifoaming agent to remove excess foam produced by the surfactant as a result of stirring the synthesis solution. The mixture was stirred for another hour before adding acetic acid until pH 11 was reached. The synthesis solution was transferred into a Teflon-lined stainless steel autoclave and hydrothermally treated at 120 °C for 3 days. After cooling to room temperature, the resulting solid was recovered by filtration, washed with deionized water and dried under ambient conditions overnight. The pre-dried powder was calcined at 550 °C for 6 h in air to remove the organic template materials. Ni-MCM-41 was synthesized via the similar procedures with nickel nitrate ($Ni(NO_3)_2 \cdot 6H_2O$, >99%, Sigma) as Ni source according to the molar ratio of $1SiO_2$:0.27Surfactant:0.26 NaOH:0.04Ni:$70H_2O$. Platinum was loaded onto the above Co- and Ni-MCM-41 materials via wet impregnation method using $H_2PtCl_4 \cdot 6H_2O$ solution.

2.2. Catalyst characterization

Powder X-ray diffraction (XRD) patterns were recorded on a Bruker AXD D8Focus diffractometer using Cu Kα radiation (λ = 0.15406 nm), operated at 40 kV and 40 mA. Nitrogen physisorption was measured on a Quantachrome Autosorb-6B at −196 °C. Before the measurement, the samples were degassed at 250 °C overnight. The surface area was obtained from multipoint BET [24] and the pore diameter was estimated from desorption branch of isotherms by the BJH method [25]. Transmission electron microscopy (TEM) image was obtained on a JEOL JEM-1400 microscope operated at 120 kV. The samples were prepared by dispersing the catalyst powder in ethanol using ultrasound, and then deposited and dried on holey carbon-coated Cu grids. Size distributions of metal particle were calculated by counting more than 200 particles at random. The reducibility of catalysts was studied by hydrogen temperature-programmed reduction (TPR) on a Quantachrome Autosorb-1C. The samples were pretreated with air at 500 °C for 60 min before reduction. All TPR profiles were recorded from 80 to 900 °C under 5% H_2 in Ar with a heating rate of 8 °C/min. Carbon formation of spent catalysts was quantitatively analyzed on a PerkinElmer Pyris Diamond TG/DTA instrument

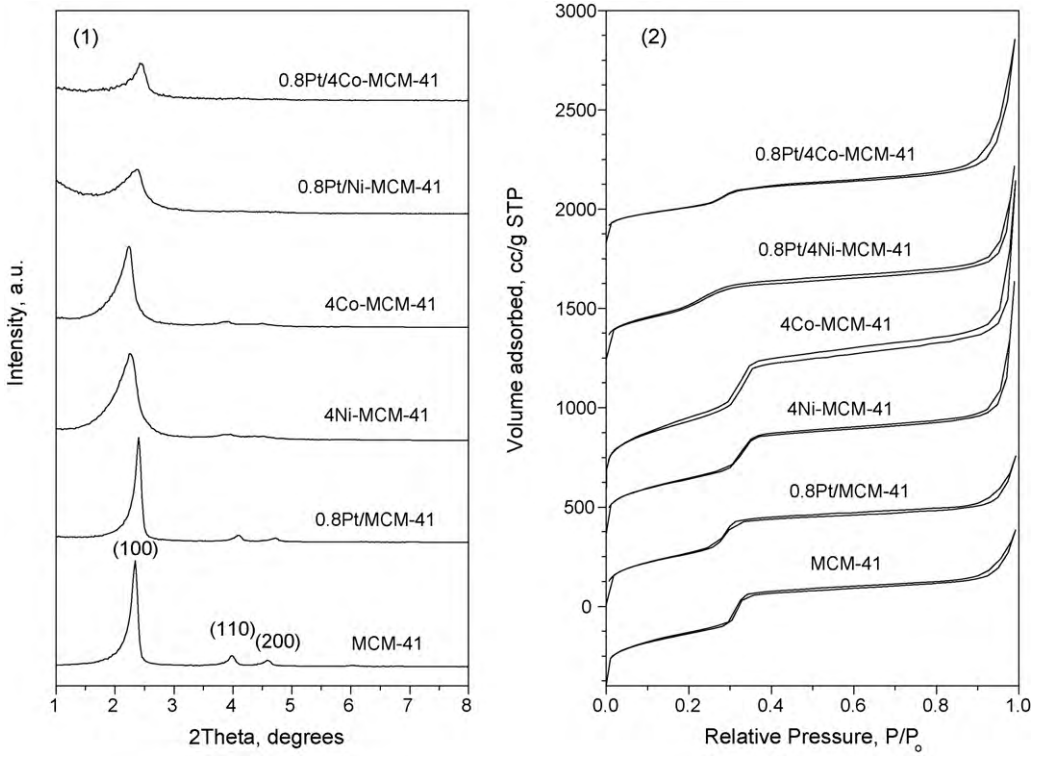

Fig. 1. (1) XRD patterns and (2) nitrogen physisorption isotherms of various MCM-41 samples.

under air atmosphere using a heating rate of 10 °C/min within a temperature range of 30–800 °C [13].

2.3. Methane dry reforming

The catalytic activity testing was carried in a fixed-bed continuous-flow reactor system under atmospheric pressure [20]. Prior to each test, the catalyst was pretreated at 750 °C for 2 h under H_2 flow. After purging with He for 1 h, a constant feed mixture CH_4/CO_2/He with molar ratio 1:1:2 was introduced into the reactor. The space velocity of feed was fixed at 50,000 mL/(h gCat). The initial activity was measured with increasing the temperature from 450 to 800 °C in the step of 50 °C. For the long-term stability test, the reaction temperature was maintained at 750 °C for 72 h on stream (TOS). The composition of the reaction products was analyzed using an on-line gas chromatograph (Agilent 6890) equipped with a Porapak Q column and a TCD. The conversions of CH_4 and CO_2, the selectivity of H_2 and CO and the ratio of CO/H_2 were calculated based on previously reported method [20].

3. Results and discussion

3.1. Characterization of fresh catalysts

The meso-structure of catalyst was identified by low angle XRD patterns (Fig. 1(1)). The intense diffraction peak at 2θ of 2.2–2.4° is assigned to the (1 0 0) diffraction. Two well resolved higher order (1 1 0) and (2 0 0) reflection peaks can also be seen for Pt impregnated and monometallic Co- and Ni-incorporated MCM-41, especially for bare MCM-41 and Pt impregnated MCM-41 samples, suggesting the highly ordered hexagonal pore structure was obtained. Nevertheless, the remarkable decrease of peak intensity was observed after impregnating Pt into Co- or Ni-incorporated MCM-41, indicating the mesoporous structures of MCM-41 become less uniform upon adding Pt onto the hetero-atom substituted MCM-41. No diffraction peaks of crystalline metal oxides were found in the XRD analysis within the 2θ range of 10–80 °C for fresh catalysts, indicating that transition metal ions are either highly dispersed in the silica framework or in the state of amorphous form outside the framework.

The mesoporous nature of all MCM-41 samples was also confirmed by nitrogen physisorption and the textural properties are listed in Table 1. The type IV isotherm pattern representative of mesoporous materials is observed as shown in Fig. 1(2) [26,27]. As the relative pressure increases, the isotherm exhibits an inflection characteristic of capillary condensation within the mesopores (P/P_o = 0.2–0.4), suggesting all the samples possess well-ordered regular pore structure. The presence of step increase at P/P_o above 0.9 is due to the macropore filling produced by inter-particle spacing. Co- and Ni-incorporated MCM-41 have higher surface area, larger pore size and volume than those of MCM-41, which indicates the incorporation of metal ions (Co, Ni) into silica framework. The pore diameter shrinks after loading Pt, which is consistent with the decrease of pore volume. This can be expected due to the partial blockage of pore channel and covering of pore wall with Pt impregnation. In comparison with siliceous MCM-41 sample, this phenomenon is more pronounced over Co-MCM-41 and Ni-MCM-41, reflecting the structural integrity of transition metal containing MCM-41 may be more sensitive to the acidic condition of impregnation.

Table 1
Textural properties of various MCM-41 samples.

Sample[a]	Surface area (m^2/g)	Pore diameter (nm)	Pore volume (cc/g)
MCM-41	948	2.65	1.85
4Co-MCM-41	1263	2.81	2.68
4Ni-MCM-41	1009	2.68	2.14
0.8Pt/MCM-41	956	2.53	1.38
0.8Pt/4Co-MCM-41	869	2.51	1.33
0.8Pt/4Ni-MCM-41	616	2.31	1.09

[a] The digit before each element denotes the nominal content of corresponding metal, wt.%.

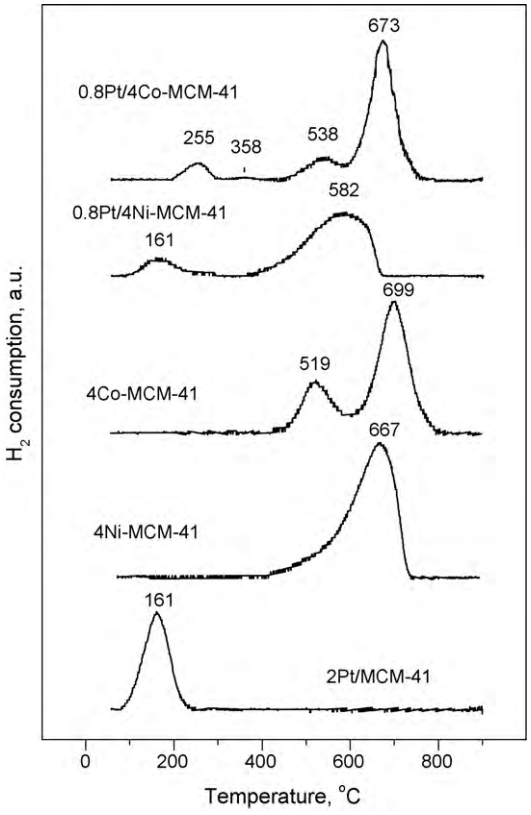

Fig. 2. TPR profiles of various MCM-41 catalysts.

The TPR profiles of transition metal containing MCM-41 catalysts are shown in Fig. 2. The reduction behaviors for these samples are remarkably different. 4Co-MCM-41 exhibits two reduction peaks at around 519 and 699 °C. As reported by Lim et al. [28], the first small peak is attributed to surface CoO_x while the second main peak corresponds to the reduction of metal ions, Co^{2+}, incorporated into silica framework of MCM-41. The presence of small amount of cobalt silicate cannot be excluded due to the high reduction temperature [29,30]. In the case of 4Ni-MCM-41, only one major reduction peak at 667 °C can be found which is assignable to the reduction of Ni^{2+} ions in the silica framework [31]. After Pt introduction, the TPR profiles exhibit marked difference. The reduction of Pt supported bimetallic catalysts occurs at lower temperatures compared with the corresponding monometallic Co- and Ni-MCM-41 catalysts. The 2 wt.% Pt impregnated MCM-41 shows a major peak at around 161 °C. It is well known that the reduction of Pt catalysts impregnated by inorganic salt takes place at temperatures below 200 °C [32–34], the rest peaks above 200 °C should mainly result from the reduction of Co or Ni ions for Pt containing Co-MCM-41 and Ni-MCM-41 samples. It has been widely reported that Pt can significantly promote the reduction of base metal (Ni or Co) [12,35–38]. Influenced by hydrogen spillover, the reduction of Co or Ni ions shift towards lower temperatures as the reduced Pt atoms can dissociate hydrogen molecules into hydrogen atoms, leading to the accelerated reduction rate of Co and Ni ions. For 0.8Pt/4Co-MCM-41, besides two reduction peaks at high temperature around

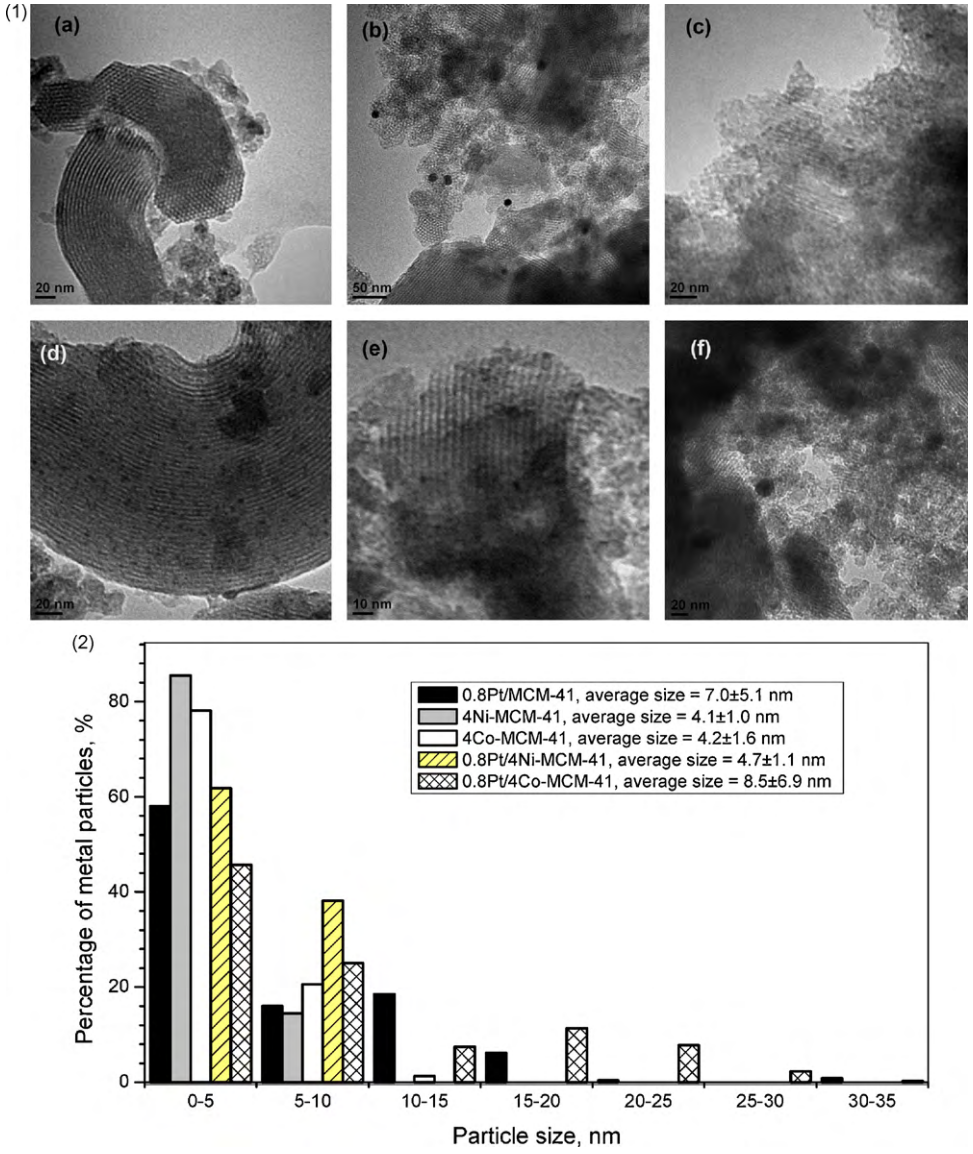

Fig. 3. (1) TEM images of the freshly pre-reduced catalysts: (a) MCM-41, (b) 0.8Pt/MCM-41, (c) 4Ni-MCM-41, (d) 4Co-MCM-41, (e) 0.8Pt/4Ni-MCM-41, and (f) 0.8Pt/4Co-MCM-41. (2) Particle size histograms of the freshly reduced catalysts.

538 and 673 °C, a low-temperature peak emerges at 255 °C followed by a broad shoulder near 358 °C. The broad reduction peak centered around 582 °C for 0.8Pt/4Ni-MCM-41 can be attributed to framework Ni^{2+} reduction; wide reduction temperature range reflects the inhomogeneous distribution of framework Ni^{2+} [31]. Noticeably, the presence of reduction peaks at moderate temperatures for 0.8Pt/4Co-MCM-41 and 0.8Pt/4Ni-MCM-41 suggests Pt–Co and Pt–Ni alloy species may form due to their close vicinity. The driving force to lower the reduction temperature of non-noble metal cations is the easier availability of more reactive hydrogen atoms in the presence of a noble metal [39] and hydrogen spillover is the involved mechanism [40]. To summarize, the addition of Pt shifts the reduction peaks of Co or Ni cations to lower temperature and may result in the formation of Pt–Co or Pt–Ni bimetallic particles [38,41].

The structural characteristics and metal particle dispersions of freshly pre-reduced catalysts were measured by TEM. As shown in Fig. 3, the honeycomb or fringe features, typical of MCM-41 are clearly seen for all the samples, which suggest the hexagonal pore channels were retained after the addition of various metal components and hydrogen pretreatment. It should be noted that during TEM observation of a 2D hexagonal sample, the honeycomb fashion emerges if the electron beam is parallel to the axes of the pores, whereas the fringe or stripes can form if the electron beam is perpendicular to the pore axis [42]. For the metal particle sizes of various metal catalysts, a larger particle size and a wider size distribution are observed on 0.8Pt/MCM-41 compared with Co- and Ni-incorporated MCM-41. Adding Pt to Co- or Ni-MCM-41 results in the increase of particle size to some extent. For instance, there are about 20% of metal particles in the size range of 15–30 nm for 0.8Pt/4Co-MCM-41. The narrow size distribution of Ni-containing catalysts suggests the metal species are well dispersed on the support surface.

3.2. Catalytic activity measurements

Initial catalytic activities of various catalysts for methane dry reforming in the temperature range of 500–800 °C are presented in Fig. 4. The methane conversion is found to increase with temperature for all the catalysts. Among three monometallic catalysts, 4Ni-MCM-41 presents the highest CH_4 conversion, followed by 0.8Pt/MCM-41 and 4Co-MCM-41 in most of the temperatures

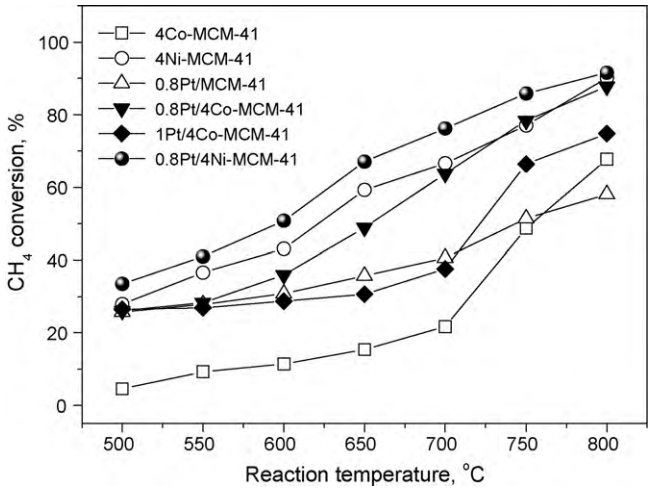

Fig. 4. Effect of temperature on CH_4 conversion over various MCM-41 catalysts.

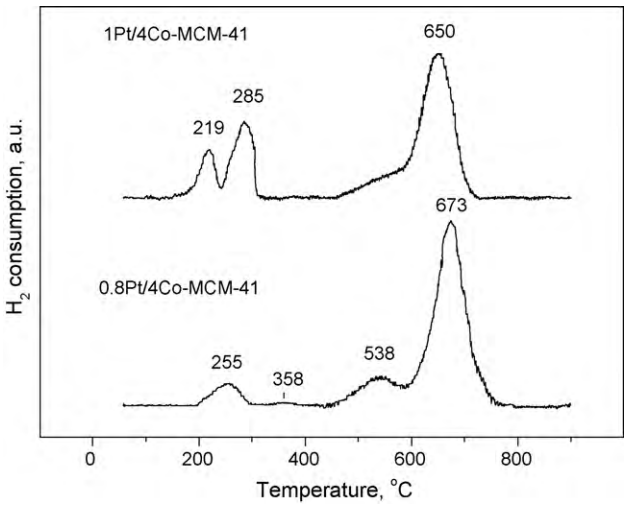

Fig. 5. TPR comparison between 0.8Pt/4Co-MCM-41 and 1Pt/4Co-MCM-41.

tested. The moderate conversion on 0.8Pt/MCM-41 is pertinent to its low metal loading, which implies less surface active sites despite the low tendency of noble metal towards carbon deposition. The impregnation of Pt has a marked influence on the initial conversion of CH_4; it is observed that both Pt impregnated Co- and Ni-MCM-41 catalysts show higher catalytic activities than the corresponding unmodified catalysts. The low reaction activity of 4Co-MCM-41 may be due to the partial oxidation of metallic Co species and/or sintering of Co particles beside the formation of carbon deposits. The oxidation of Co catalysts was observed during CO_2 reforming of CH_4 [43–45]. The oxidation of Co species is related with the low Co content (for instance, <9 wt.%) along with the coexistence of reductive (CH_4, H_2) and oxidative (CO_2) components [45]. To explain the remarkable activity difference between 0.8Pt/4Co-MCM-41 and 1Pt/4Co-MCM-41, TPR characterization was further conducted (Fig. 4). As Pt content increases from 0.8 to 1 wt.%, two low-temperature reduction peaks at 219 and 285 °C appear, implying the increased surface interaction between Pt and Co species. The strong Pt–Co interaction over 1Pt/4Co-MCM-41 may lead to a Co-enriched metal surface due to the lower vaporization enthalpy of cobalt (377 kJ mol^{-1}) than that of platinum (469 kJ mol^{-1}) [46]. The excessive Co species on the surface may partially counteract the improvement effect of Pt species. In this study, the preferable Pt loading is 0.8 wt.% for both 4Co-MCM-41 and 4Ni-MCM-41 catalysts. Using these catalysts, a better carbon-resistance is expected; also the suppression of metal sintering could be enhanced. As the Pt content increases to 1 wt.%, extensive metal sintering induced by Pt reduction may occur, thus decreasing the catalytic activity. Noticeably, the initial conversion of CH_4 over 0.8Pt/4Ni-MCM-41 is better than that of 0.8Pt/4Co-MCM-41 at all the tested temperatures. Fig. 5

To illustrate the effect of Pt introduction on long-term catalytic stability, a constant temperature experiment was carried out at 750 °C for 72 h and the obtained results are shown in Fig. 6. A significant feature is that adding 0.8 wt.% Pt remarkably enhances the catalytic activity and stability, especially for 0.8Pt/4Ni-MCM-41, which shows the best CH_4 conversion and catalytic stability. Although the initial activity of monometallic 4Co- and 4Ni-MCM-41 is around 66%, they experience the rapid deactivation. The average deactivation rate of these catalysts has the following sequence (%h^{-1}): 4Co-MCM-41 ~ 4Ni-MCM-41 (4.0) > 0.8Pt/4Co-MCM-41 (0.7) > 0.8Pt/MCM-41 (0.1) > 0.8Pt/4Ni-MCM-41 (0.0). The deactivation rate of monometallic Ni-MCM-41 catalyst is much faster than the results we reported previously [13,15], and the reason can be related with the different synthesis procedures of MCM-41 catalyst. In this study, NaOH was introduced in order to elevate the pH level of synthesis solution. As reported by Lim et al. [47], adding impurities to the pure silica synthesis solution results in the shift of the maximum reduction rate of metal ions to lower temperature. They suggested it might be due to the competition between impurity and metal ions for the substitution sites. The inferior structural stability was also found on MCM-41 assembled from sodium silicate or adding 0.1% Na_2O to synthesis gel, which confirms the deleterious effect of sodium [48].

3.3. Deactivation analysis

Carbon deposits over the spent catalysts after stability test were analyzed by TGA under air atmosphere and the results are shown in Fig. 7. One can observe a distinct broad hump during the weight loss of 0.8Pt/4Ni-MCM-41 within the temperature range of 320–630 °C, which can be ascribed to the oxidation of metallic Ni, Pt, or Ni–Pt particles. This result strongly suggests more active metal sites are formed over 0.8Pt/4Ni-MCM-41 catalyst. The average carbon deposition (% g^{-1} h^{-1}) changes as follows: 4Co-MCM-41 (1.62) > 4Ni-MCM-41 (1.14) > 0.8Pt/4Co-MCM-41 (0.28) > 0.8Pt/MCM-41 (0.20) > 0.8Pt/4Ni-MCM-41 (0.11). This sequence of weight loss is consistent with the trend of catalytic

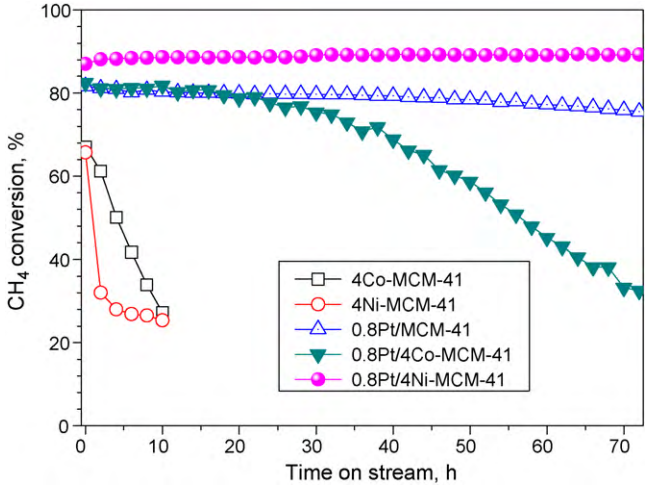

Fig. 6. The stability test of various MCM-41 catalysts.

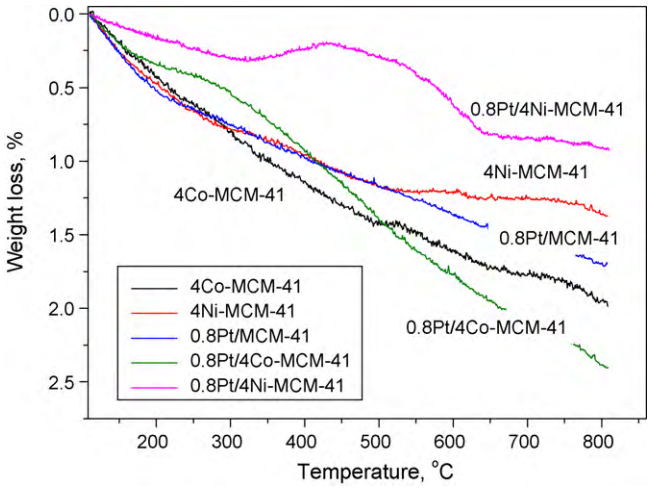

Fig. 7. TG of spent MCM-41 catalysts after stability test.

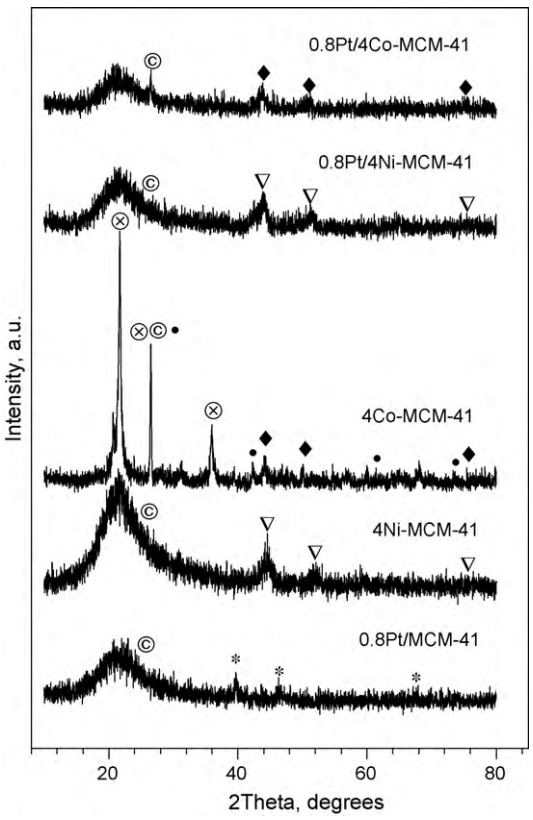

Fig. 8. XRD patterns of the spent MCM-41 catalysts. (Crystalline phase: (1) (*), Pt; (2) (▽), Ni; (3) (♦), Co; (4) (●), CoO; (5) (⊗), crystalline SiO_2; (6) (©), graphite.

activity in the long-term stability test on the whole. These results indicate that the presence of a small quantity of noble metal Pt can effectively alleviate the deposition of carbon over active metal surface. The higher rate of carbon deposition over cobalt catalyst may be due to the facile formation of highly hydrogen-deficient hydrocarbon species [49]. A moderate carbon deposition was observed on 0.8Pt/MCM-41, though it is generally granted that supported noble metal catalysts have high selectivity for carbon-free operation than Ni [50]. Nevertheless, carbon formation does occur on noble metal, depending upon the nature of support and the metal particle size [51]. The essential reason for this deactivation can also be explained as the carbonaceous species generated from methane dissociation cannot be timely depleted via chemisorbed CO_2 oxidation. We also suggest the synergetic interaction between Pt and Ni/Co plays an important role in maintaining high activity of metal active sites and reducing the carbon formation. Similar promotion effect of noble metal was also observed in previous studies [12,13,16,41,44].

The crystalline phase composition of the used catalysts after stability test was investigated by XRD. As shown in Fig. 8, all the spent samples except 4Co-MCM-41 exhibit a dispersed diffraction centered around 22° due to the amorphous silica. Zero-valent metal, Ni and Co can be detected for the corresponding MCM-41 catalysts. Because of the low Pt content and XRD detect limitation, no significant diffraction peaks of Pt are found, and it is also rather difficult to find bimetallic alloy particle. Graphitic carbon is observed for the spent catalysts, though its diffraction would be partly shielded by the relatively strong signal of amorphous silica. In contrast to other catalysts, the used 4Co-MCM-41 shows significant crystalline phases of SiO_2, such as quartz and tridymite. Furthermore, cobalt oxide (CoO) and a small quantity of cobalt silicate are also detected. These multiple crystalline transformations during the reaction are closely associated its inferior catalytic activity. Fortunately this deleterious effect can be suppressed by adding an appropriate amount of Pt. The amorphous nature of silica species over the used 0.8Pt/4Co-MCM-41 after 72 h reaction well attests to the beneficial influence of Pt addition.

The metal particle sizes and size distributions of the deactivated catalysts are shown in Fig. 9 (also see TEM of the fresh reduced catalysts for comparison). For 0.8Pt/MCM-41 catalyst, a significant sintering of Pt nanoparticles is present, it shows a broad particle distribution, 13% of metal particles being larger than 30 nm though most of Pt particles are situated between 0.8 and 32 nm. The large Pt particles are responsible for the deactivation of the catalyst to some extent because graphite-like deposits are indeed observed on the used 0.8Pt/MCM-41. A small particle size and narrow distribution are observed for 4Ni-MCM-41, being the smallest average particle size of 8.3 nm among all the used catalysts. However, its catalytic behavior is not as good as anticipated, one possible explanation is that the accessibility of metal particles is blocked considerably, for instance, the metallic particles are occluded by silica matrix. Another reason could be the activation ability of the metallic particles are weakened by electronic effect, the presence of small quantity of unreduced Ni^{2+} species result in the formation of the electron-deficient metallic Ni species, which was widely observed over zeolite supported noble metal catalysts [52,53]. For 4Co-MCM-41 catalyst, the average metal particle size is 16.1 nm, much larger than that of 4Ni-MCM-41, also 2.8 fold higher than that of freshly reduced 4Co-MCM-41, suggesting the obvious metal sintering occurs accompanied by the crystalline transformation of silica matrix during the reaction. The average metal particle sizes become larger after introducing Pt to Ni- or Co-MCM-41 compared to the corresponding monometallic Ni- or Co-MCM-41 and the freshly reduced 0.8Pt/4Ni- or 4Co-MCM-41. Nevertheless, the spent 0.8Pt/4Ni-MCM-41 still possesses a smaller particle size and relatively narrower distribution than the spent 0.8Pt/4Co-MCM-41, which explains the superior catalytic activity and stability of 0.8Pt/4Ni-MCM-41. Due to the presence of parasitical reaction of CH_4 decomposition and CO disproportionation, carbon formation over the catalyst surface is inevitable. From TEM image (f), one can clearly see the filamentous carbon structures, despite its lowest trend of carbon formation. In summary, some increase of metal particle size occurs after Pt addition; though it does not affect its positive effect on the enhancement of catalytic activity. A suitable combination of Pt and Ni (or Co) can provide sufficient metal centers with high dispersion under reaction conditions, therefore maintaining a high catalytic activity and restraining carbon deposition.

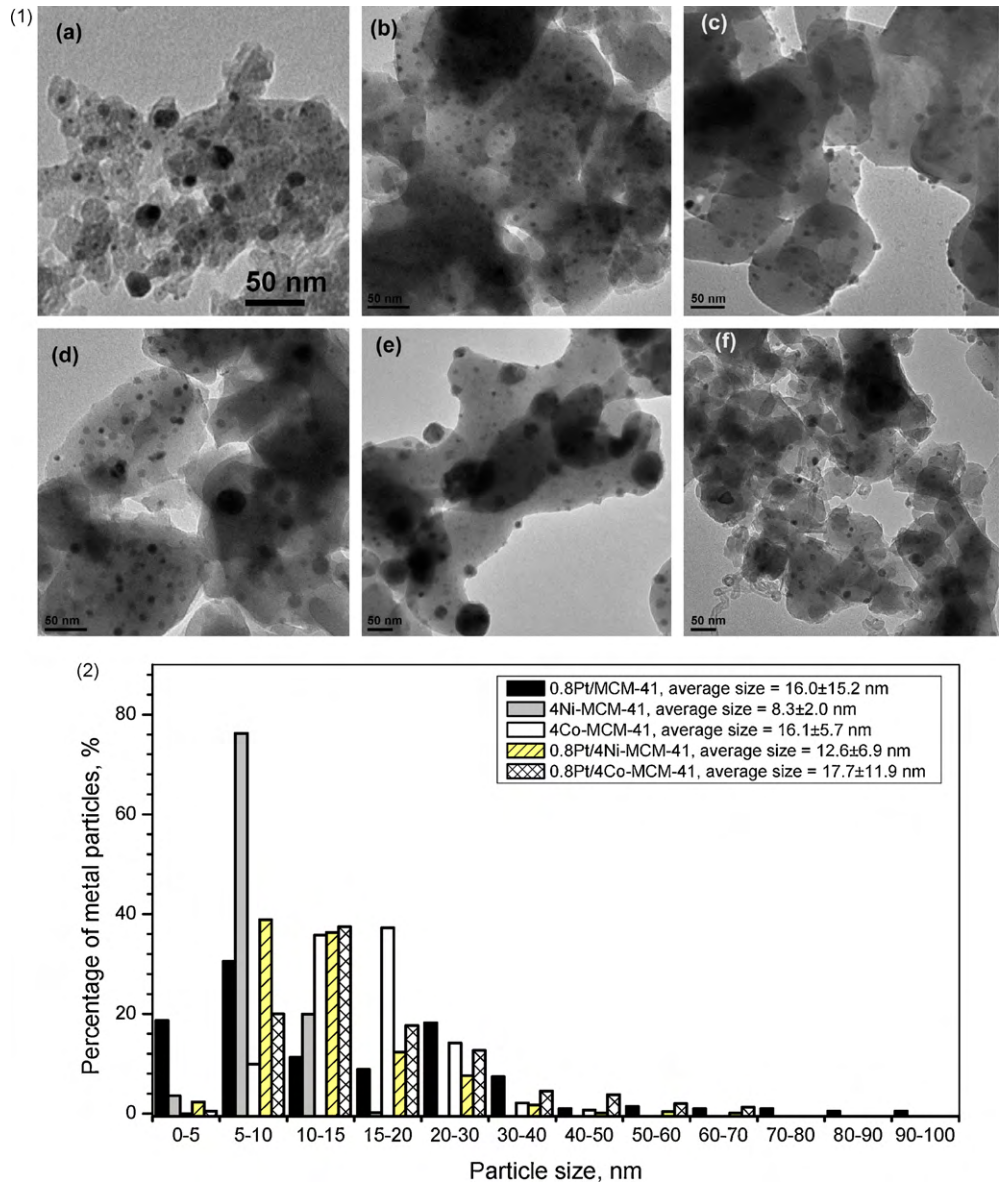

Fig. 9. (1) TEM images of the used catalysts: (a) 0.8Pt/MCM-41, (b) 4Ni-MCM-41, (c) 4Co-MCM-41, (d) 0.8Pt/4Ni-MCM-41, (e) 0.8Pt/4Co-MCM-41, and (f) a typical carbon deposited on the used 0.8Pt/4Ni-MCM-41. (2) Particle size histograms of the used catalysts.

4. Conclusions

Two transition metal (Co- and Ni-) based MCM-41 catalysts, promoted with Pt were prepared and evaluated for CH_4 reforming with CO_2 under atmospheric pressure. The noble metal Pt was found to serve as a good promoter and active component, especially a high activity and excellent stability were achieved over 0.8Pt/4Ni-MCM-41 catalyst. The larger particle size was observed for both Pt impregnated Co- and Ni-MCM-41 catalysts. The comparative study results showed the deactivation behaviors varied over different catalysts. Accelerated deactivation occurred in the presence of sodium impurity for monometallic Co- and Ni-MCM-41 catalysts. The significant increase of metal particle size over 0.8Pt/4Co-MCM-41 resulted in its activity loss with time on stream considerably. The beneficial effect of Pt addition is believed to be contributed to its lower tendency to carbon deposition. TPR results showed a special interaction between Pt and Co or (Ni) in these catalysts, the presence of this hydrogen spillover effect can lead to the formation sufficient metallic active sites with high durability thus facilitating the improvement of catalytic performance.

Acknowledgements

The authors thank AcRF tier 2 (ARC 13/07) for providing funding support. The financial support of A*STAR project 062 101 0035 is also gratefully acknowledged.

References

[1] C.S. Song, Catal. Today 115 (2006) 2.
[2] M.C.J. Bradford, M.A. Vannice, Catal. Rev. Sci. Eng. 41 (1999) 1.
[3] F. Kapteijn, J. Rodriguez-Mirasol, J.A. Moulijn, Appl. Catal. B: Environ. 9 (1996) 25.
[4] F. Fischer, H. Tropsch, Brennst. Chem. 39 (1928).
[5] J.R.H. Ross, A.N.J. van Keulen, M.E.S. Hegarty, K. Seshan, Catal. Today 30 (1996) 193.
[6] I. Wender, Fuel Process. Technol. 48 (1996) 189.
[7] J.R. Rostrup-Nielsen, J.-H. Bak Hasen, J. Catal. 144 (1993) 38.
[8] J.T. Richardson, S.A. Paripatyadar, Appl. Catal. 61 (1990) 293.
[9] J.R. Rostrup-Nielsen, J-H.B. Hansen, J. Catal. 144 (1993) 38.
[10] E. Ruckenstein, H.Y. Wang, J. Catal. 205 (2002) 289.
[11] Y.H. Hu, E. Ruckenstein, Adv. Catal. 48 (2004) 297.
[12] Y.G. Chen, K. Tomishige, K. Yokoyama, K. Fujimoto, Appl. Catal. A 165 (1997) 335.
[13] W.K. Jóźwiak, M. Nowosielska, J. Rynkowski, Appl. Catal. A 280 (2005) 233.

[14] A.N. Pinheiro, A. Valentini, J.M. Sasaki, A.C. Oliveira, Appl. Catal. A 355 (2009) 156.
[15] C. Crisafulli, S. Scirè, S. Minicò, L. Solarino, Appl. Catal. A 225 (2002) 1.
[16] F. Besenbacher, I. Chorkendorff, B.S. Clausen, B. Hammer, A.M. Molenbroek, J.K. Nørskov, I. Stensgarrd, Science 279 (1998) 1913.
[17] A.M. Molenbroek, J.K. Nørskov, B.S. Clausen, J. Phys. Chem. B 105 (2001) 5450.
[18] J.C. Vartuli, S.S. Shih, C.T. Kresge, J.S. Beck, Stud. Surf. Sci. Catal. 117 (1998) 13.
[19] A. Corma, Chem. Rev. 97 (1997) 2373.
[20] D. Liu, R. Lau, A. Borgna, Y. Yang, Appl. Catal. A 358 (2009) 110.
[21] D. Liu, X.-Y. Quek, H.H. Adeline, G. Zeng, Y. Li, Y. Yang, Catal. Today 148 (2009) 243.
[22] D. Liu, X.Y. Quek, W.N.E. Cheo, R. Lau, A. Borgna, Y. Yang, J. Catal. 266 (2009) 380.
[23] S. Lim, D. Ciuparu, C. Pak, F. Dobek, Y. Chen, D. Harding, L. Pfefferle, G.L. Haller, J. Phys. Chem. B 107 (2003) 11049.
[24] S. Brunauer, P.H. Emmett, E. Teller, J. Am. Chem. Soc. 60 (1938) 309.
[25] E.P. Barrett, L.G. Joyner, P.P. Halenda, J. Am. Chem. Soc. 73 (1951) 373.
[26] J. Brunaur, L.S. Deming, W.E. Deming, E. Teller, J. Am. Chem. Soc. 62 (1940) 1723.
[27] K.S.W. Sing, D.H. Evertt, R.A.W. Haul, L. Moscou, R.A. Pierrotti, J. Rouduerol, T. Siemieniewska, J. Pure Appl. Chem. 57 (1985) 603.
[28] S. Lim, D. Ciuparu, Y. Yang, G. Du, L. Pfefferle, G.L. Haller, Micropor. Mesopor. Mater. 101 (2007) 200.
[29] G.J. Haddad, J.G. Goodwin Jr., J. Catal. 157 (1995) 25.
[30] S. Lim, D. Ciuparu, Y. Chen, L. Pfefferle, G.L. Haller, J. Phys. Chem. B 108 (2004) 20095.
[31] Y. Yang, S. Lim, G. Du, Y. Chen, D. Ciuparu, G.L. Haller, J. Phys. Chem. B 109 (2005) 13237.
[32] I. Sobczak, M. Ziolek, M. Nowacka, Micropor. Mesopor. Mater. 78 (2005) 103.
[33] N. Yao, C. Pinckney, S. Lim, C. Pak, G.L. Haller, Micropor. Mesopor. Mater. 44 (2001) 377.
[34] J.M. Rynkowski, T. Paryjczak, M. Lenik, M. Farbotko, J. Góralski, J. Chem. Soc. Faraday Trans. 91 (1995) 3481.
[35] A. Tanksale, J.N. Beltramini, J.A. Dumesic, G.Q. Lu, J. Catal. 258 (2008) 366.
[36] C. Raab, J.A. Lercher, J.G. Goodwin Jr., J.Z. Shyu, J. Catal. 122 (1990) 406.
[37] G. Jacobs, Y.Y. Ji, B.H. Davis, D. Cronauer, A.J. Kropf, C.L. Marshall, Appl. Catal. A 333 (2007) 177.
[38] L. Gutierrez, E.A. Lombardo, J.O. Petunchi, Appl. Catal. A 194 (2000) 169.
[39] A. Jentys, B.J. McHugh, G.L. Haller, J.A. Lercher, J. Phys. Chem. 96 (1992) 1324.
[40] W.C. Conner, J.L. Falconer, Chem. Rev. 95 (1995) 759.
[41] B. Pawelec, S. Damynova, K. Arishtirova, J.L.G. Fierro, L. Petrov, Appl. Catal. A 323 (2007) 188.
[42] A. Chenite, Y. Le Page, A. Sayari, Chem. Mater. 7 (1995) 1015.
[43] K. Takanabe, K. Nagaoka, K. Nariai, K. Aika, J. Catal. 232 (2005) 268.
[44] K. Nagaoka, K. Takanabe, K. Aika, Appl. Catal. A 268 (2004) 151.
[45] E. Ruchenstein, H.Y. Wang, J. Catal. 205 (2002) 289.
[46] J.G. Speight, Lange's Handbook of Chemistry, 16th ed., McGraw-Hill, New York, 2005.
[47] S.Y. Lim, Y.H. Yang, D. Ciuparu, C. Wang, Y. Chen, L. Pfefferle, G.L. Haller, Top. Catal. 34 (2005) 31.
[48] T.R. Pauly, V. Petkov, Y. Liu, S.J.L. Billinge, T.J. Pinnavaia, J. Am. Chem. Soc. 124 (2002) 97.
[49] T. Osaki, H. Masuda, T. Horiuchi, T. Mori, Catal. Lett. 34 (1995) 59.
[50] T. Inui, Catalysis, vol. 16, The Royal Society of Chemistry, Cambridge, 2002, p. 133.
[51] J.H. Bitter, K. Seshan, J.A. Lercher, J. Catal. 183 (1999) 336.
[52] W.M.H. Sachtler, A.Y. Stakheev, Catal. Today 12 (1992) 283.
[53] R.A. Dalla Betta, M. Boudart, in: H. Hightower (Ed.), Proceedings of the 5th International Congress on Catalysis, North Holland, Amsterdam, 1973, p. 1329.